



Reductive dechlorination of 2,4-dichlorophenol by Pd/Fe nanoparticles prepared in the presence of ultrasonic irradiation

Deming Zhao^a, Min Li^{a,c}, Dexing Zhang^a, Shams Ali Baig^b, Xinhua Xu^{b,*}

^a College of Chemical Engineering and Materials Science, Zhejiang University of Technology, Hangzhou 310032, PR China

^b College of Environmental and Resource Sciences, Zhejiang University, Hangzhou 310058, PR China

^c Ningbo Research and Design Institute of Chemical Industry, Ningbo 315040, PR China

ARTICLE INFO

Article history:

Received 15 August 2012

Received in revised form 29 October 2012

Accepted 25 November 2012

Available online 3 December 2012

Keywords:

2,4-DCP
Reductive dechlorination
Pd/Fe nanoparticles
Ultrasound
Kinetics

ABSTRACT

Palladium/Iron (Pd/Fe) nanoparticles were prepared by using ultrasound strengthened liquid phase reductive method to enhance dispersion and avoid agglomeration. The dechlorination of 2,4-dichlorophenol (2,4-DCP) by Pd/Fe nanoparticles was investigated to understand its feasibility for an in situ remediation of contaminated groundwater. Results showed that 2,4-DCP was first adsorbed by Pd/Fe nanoparticles, then quickly reduced to o-chlorophenol (o-CP), p-chlorophenol (p-CP), and finally to phenol (P). The induction of ultrasound during the preparation of Pd/Fe nanoparticles further enhanced the removal efficiency of 2,4-DCP, as a result, the phenol production rates increased from 65% (in the absence of ultrasonic irradiation) to 91% (in the presence of ultrasonic irradiation) within 2 h. Our data suggested that the dechlorination rate was dependent on various factors including Pd loading percentage over Fe⁰, Pd/Fe nanoparticles availability, temperature, mechanical stirring speed, and initial pH values. Up to 99.2% of 2,4-DCP was removed after 300 min reaction with these conditions: Pd loading percentage over Fe⁰ 0.3 wt.%, initial 2,4-DCP concentration 20 mg L⁻¹, Pd/Fe dosage 3 g L⁻¹, initial pH value 3.0, and reaction temperature 25 °C. The degradation of 2,4-DCP followed pseudo-first-order kinetics reaction and the apparent pseudo-first-order kinetics constant was 0.0468 min⁻¹.

© 2012 Elsevier B.V. All rights reserved.

1. Introduction

Chlorinated phenols (CPs) have been widely used in the production of wood preservers, pesticides, dyestuffs, lubricants, dielectric and biocides, that is why found in nearly all major environmental components [1]. Most of them are toxic, carcinogenic, and bio-refractory [2,3]. Moreover, they could persist in the environment for a long time, and do harm to human health by bioaccumulation [4]. Due to the aryl structure and the presence of chlorine atom, chloroaromatics are exceptionally recalcitrant towards chemical reactions aimed at their destruction [2]. This raises an urgent need for efficient reductive dechlorination methods to eliminate chloroaromatics from both concentrated industrial effluents and diluted polluted groundwater.

Zero-valent iron (Fe⁰, ZVI) is a mild reducing agent with reduction potential of -0.440 V. Treatment of recalcitrant chemicals using Fe⁰ has been a main focus of researches in recent years [1–3,5]. A rapid and complete reductive dechlorination technology of chloroaromatics involving the use of bimetallic Pd/Fe nanoparticles that led to the formation of non-chlorinated hydrocarbons have also been reported [1,3,6]. As one of the noble metal, Pd can

utilize the produced H₂ from Fe⁰ corrosion and accelerate the rates of dechlorination reaction [7,8]. However, the presence of Pd not only reduces the accumulation of toxic byproducts, but also inhibits particle oxidation in air [9]. Pd/Fe bimetallic nanoparticles, when compared to the conventional large particles have some advantages with possessing large specific surface area and high surface reactivity [10].

In order to obtain the stabilized and high reactive Pd/Fe bimetallic nanoparticles and decrease their agglomeration and accumulation in the effluent, ultrasound is applied to the preparation of Pd/Fe bimetallic nanoparticles. Sono-chemistry arises from acoustic cavitation, the formation, growth, and implosive collapse of bubbles in a liquid. Acoustic cavitation can increase the surface area of the reactive solids by causing particles to rupture [10,11].

In the present work, an attempt has been made to prepare Pd/Fe bimetallic nanoparticles with the help of sonication for better dispersion and also avoiding the agglomeration. The performance of bimetallic systems in the remediation of contaminated groundwater under ambient condition, the dechlorination of 2,4-DCP by nanoscale Pd–Fe particles was investigated. In addition, other factors contributing to 2,4-DCP reduction, such as Pd/Fe nanoparticles dosage, Pd loading percentage over Fe⁰, initial 2,4-DCP concentration, mechanical stirring speed and initial pH values, were also examined.

* Corresponding author. Tel./fax: +86 571 88982031.

E-mail address: xuxinhua@zju.edu.cn (X. Xu).

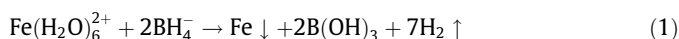
2. Experimental

2.1. Chemicals

Iron sulfate heptahydrate (AR grade), 2,4-DCP (chemically pure, or AP grade), o-CP (CP grade), p-CP (CP grade), phenol (CP grade) were purchased from the Sinopharm Group Chemical Reagent Co., Ltd., China, Potassium hexachloropalladate (K_2PdCl_6 , 99%) obtained from Aladdin-Reagent. Sodium borohydride (AR grade) purchased from Tianjin Chemical Reagent Institute. All chemicals were used as received without further purification. 2,4-DCP is dissolved in deionized water and stored at 4 °C. Pd/Fe nanoparticles were synthesized immediately before use.

2.2. Synthesis

In the presence or absence of 20 kHz and 150 W KQ-3200DB ultrasonic elutriation apparatus with effective volume of 2000 mL purchased from Kunshan ultrasonic apparatus Co., Ltd., China, Pd/Fe bimetallic nanoparticles were prepared in a 500 mL three-necked flask under nitrogen gas. Fe^0 nanoparticles were synthesized by drop wise addition of stoichiometric amounts of $NaBH_4$ (0.50 mol L^{-1}) aqueous solution into a flask containing $FeSO_4 \cdot 7H_2O$ (0.25 mol L^{-1}) aqueous solution simultaneously with mechanical stirring at 25 °C by external circulation at low temperature water cooling system. The ferrous iron was reduced to zero-valent iron according to the following reaction:



The Fe^0 nanoparticles were then rinsed several times with deoxygenated deionized water. Subsequently, Pd/Fe nanoparticles were prepared by reacting with the wet Fe^0 nanoparticles in an aqueous solution of potassium hexachloropalladate (6.13 mmol L^{-1}) under mechanical stirring according to the following equation:



2.3. Batch experimental procedures

Batch experiments of 2,4-DCP dechlorination were performed in the same three-necked flask into which Pd/Fe nanoparticles were added. 2,4-DCP stock solutions and a certain amount of deoxygenated deionized water were added into the flask containing freshly prepared Pd/Fe nanoparticles into 500 mL of total reaction volume. The reaction solution was stirred under nitrogen flow to simulate anaerobic environment at 25 °C. Aliquots of samples were periodically collected with glass syringes and the reaction was quenched by passing through $0.22 \mu\text{m}$ polyether sulphone (PES) membrane filters.

2.4. Methods of analysis

Prior to the characterization, all freshly synthesized Pd/Fe nanoparticles (with a Pd bulk loading of 0.3%) were immersed in absolute ethyl alcohol and dispersed by an ultrasonicator. Brunauer–Emmett–Teller (BET) specific surface area of all synthesized Pd/Fe nanoparticles were measured using nitrogen adsorption method with a surface analyzer (ASAR2020M+, Micromeritics Instrument Corp., US). Before the analysis, the particles were dried in vacuum at 25 °C for 24 h and then hydrogen flow at 260 °C for further 4 h. Transmission electron microscope (TEM) images of the particles were obtained with a JEOL JEM 200CX microscope (JEOL Electronics Co., JP) performed at a voltage of 160 kV for morphological measurements. Scanning electron microscope (SEM) images were obtained through a microscope (HITACHI S-4800

HITACHI Instruments Corp., JP). X-ray diffraction (XRD) analysis was performed by using X'Pert Pro advanced X-ray diffractometer ($\lambda = 1.5418 \text{ \AA}$).

Organic compounds such as 2,4-DCP, p-CP, o-CP and phenol were analyzed by SHIMADZU High Performance Liquid Chromatography. Agilent C18 Column, $150 \times 4.6 \text{ mm}$, mobile phase: MeOH/ H_2O (60/40, v/v), flow rate: 1.0 mL min^{-1} , detector: UV at 280 nm, sample size: 20 μL .

3. Results and discussion

3.1. Characterization of Pd/Fe nanoparticles

The BET specific surface area of the synthesized Pd/Fe nanoparticles in the presence and absence of 20 kHz ultrasonic irradiation were 37.77 and $22.39 \text{ m}^2 \text{ g}^{-1}$, respectively. Fig. 1(a)–(c) shows TEM images of the freshly prepared Pd/Fe nanoparticles in the presence and absence of ultrasonic irradiation, and the reacted (after 300 min) Pd/Fe nanoparticles prepared in the presence of ultrasound. The freshly prepared Pd/Fe nanoparticles in the absence of ultrasound, were spherical in shape with particle size ranging from 20 to 100 nm, and appeared to aggregate together (Fig. 1(a)). However, Pd/Fe nanoparticles prepared in the presence of ultrasound were also spherical, but the particle size ranges from 10 to 100 nm, and appeared to be smaller particles diameter and better dispersion (Fig. 1(b)). Spherical particles aggregate to form dendrites due to geomagnetic forces between nanoscale particles and small particles, and also their surface tension interactions [12,13]. A mucous layer was adhered onto the surface of Pd/Fe nanoparticles prepared in the absence of ultrasound, reflects the possibility of lowering the dechlorination efficiency. A thickly mucous layer was showed on the surface of the Pd/Fe nanoparticles prepared in the presence of ultrasound after 300 min of reaction (Fig. 1(c)). More organic components such as phenol and 2,4-DCP, as well as metal hydroxides and carbonate passivating layers on the nanoparticles' surface inhibited the particles' active sites, likely leading to lower dechlorination efficiency. The SEM images of the fresh Pd/Fe nanoparticles prepared in the presence of ultrasound, and the reacted (after 300 min) Pd/Fe nanoparticles prepared in presence of ultrasound are shown in Fig. 1(d) and (e). Fig. 1(d) shows many Pd particles loaded on the surface of Pd/Fe nanoparticles. After 300 min of reaction, Pd particles loaded on the surface of Pd/Fe nanoparticles decreased and the white platelet-shaped crystals appeared (Fig. 1(e)), suggests the formation of iron oxides resulting from iron corrosion in water. These minerals were likely composed of goethite ($\alpha\text{-FeOOH}$) or lepidocrocite ($\gamma\text{-FeOOH}$) [3,14,15]. Huang and Zhang [15] also suggested that a stratified ZVI corrosion coating would form in water, for which the outer and middle layers comprised both $FeOOH$ and Fe_3O_4 , while the inner layer mainly consisted of Fe_3O_4 . This is generally consistent with our observation in XRD patterns. Fig. 1(f) shows the XRD patterns of the fresh and the 300 min aged Pd/Fe nanoparticles prepared in the presence of ultrasound. The XRD pattern for the fresh sample presents a strong peak 44.66° which corresponds to the body-centered cubic $N\text{-Fe}^0$ at the (110) plane. The peak in the XRD pattern of the aged sample shows evidence of iron oxides, possibly Fe_3O_4 (magnetite) or Fe_2O_3 (maghemite), or their mixture. This agrees with the fact that Fe^0/Fe_3O_4 couple is more thermodynamically favorable at pH above 6.1 [18].

3.2. Comparisons on 2,4-DCP reductive dechlorination by Pd/Fe nanoparticles prepared in the presence and absence of ultrasonic irradiation

Effects of different Pd/Fe nanoparticles synthesized methods on 2,4-DCP reductive dechlorination were investigated at Pd/Fe

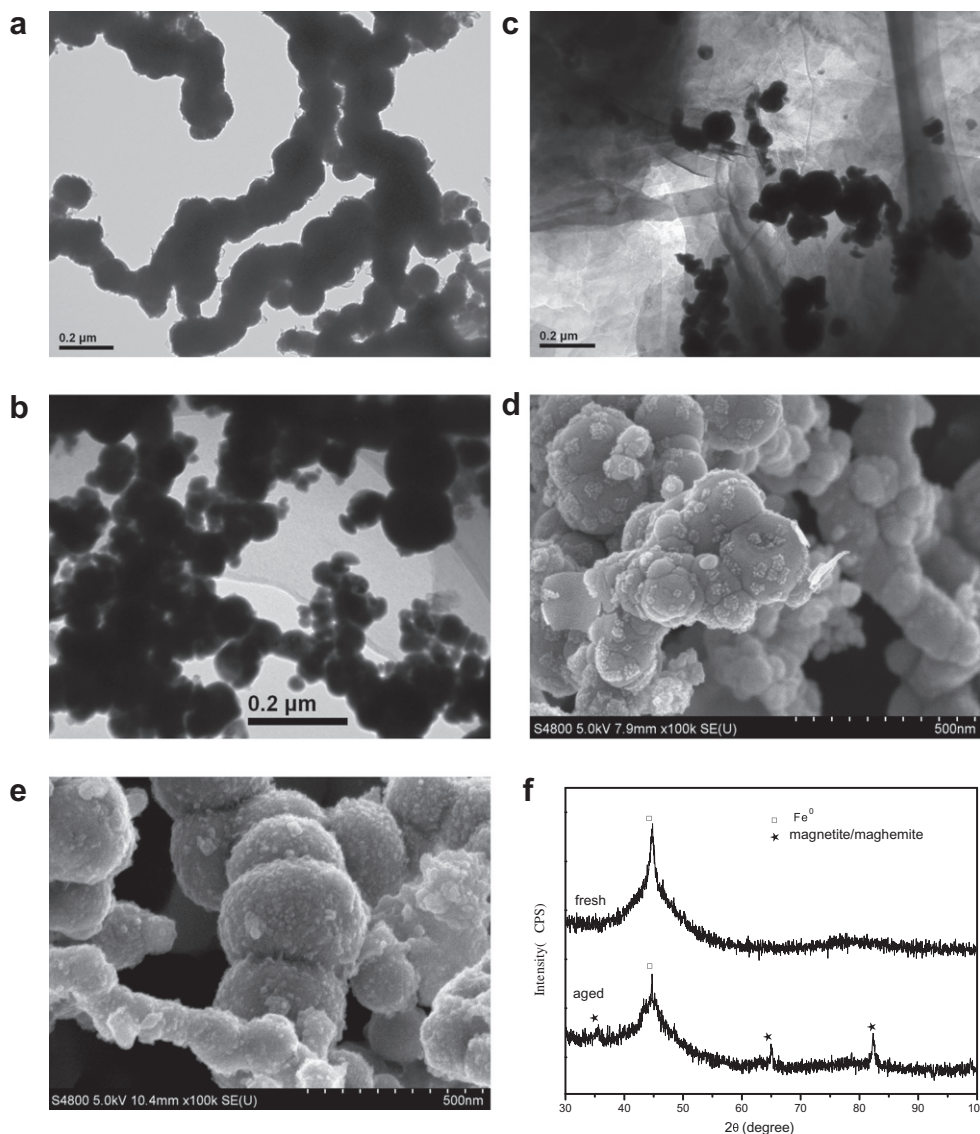


Fig. 1. (a) TEM image of fresh Pd/Fe nanoparticles prepared in the absence of ultrasonic irradiation, (b) TEM image of fresh Pd/Fe nanoparticles prepared in the presence of ultrasonic irradiation, (c) TEM image of aged Pd/Fe nanoparticles prepared in the presence of ultrasonic irradiation, (d) SEM image of fresh Pd/Fe nanoparticles prepared in the presence of ultrasonic irradiation, (e) SEM image of aged Pd/Fe nanoparticles prepared in the presence of ultrasonic irradiation (300 min) and (f) XRD patterns of fresh and aged Pd/Fe nanoparticles prepared in the presence of ultrasonic irradiation.

nanoparticles dosage of 3 g L^{-1} , the Pd loading percentage over Fe^0 of 0.3 wt.%, initial 2,4-DCP concentration of 20 mg L^{-1} , an initial pH value of 3.0, reaction temperature of $25 \text{ }^\circ\text{C}$ and mechanical stirring speed of 400 rpm. Fig. 2 shows reductive dechlorinations of 2,4-DCP by Pd/Fe nanoparticles synthesized in the presence and absence of ultrasonic irradiation.

2,4-DCP was first adsorbed by Pd/Fe nanoparticles, then reduced to o-CP and p-CP, and later converted to phenol, as a sole final organic product. No other chlorinated intermediates or final organic products were detected. The concentration of 2,4-DCP decreased rapidly and the removal percentage reached 94% in 180 min, then further improved to nearly 98% in 300 min for Pd/Fe nanoparticles synthesized in the presence of ultrasound. In contrast, only about 70% and 85% of the removal percentage were obtained for Pd/Fe nanoparticles synthesized in the absence of ultrasound during the same reaction periods, respectively. Phenol and inorganic chlorine were detected as the final products in the dechlorination reaction. Compared to initial concentration (20 mg L^{-1} 2,4-DCP), so approximately 17–27% carbon mass losses

were observed. This indicates that a fraction of organic compounds was absorbed or covered by surface passivating layers due to the precipitation of metal hydroxides on the surface of iron and Pd/Fe particles. This is also evidenced by the fact that the 2,4-DCP concentration dropped rapidly in the first 15 min, but the phenol being generated was much less than the maximum attainable. The non-detected fraction of intermediates may be associated with Pd/Fe nanoparticles, which appear to serve as non-reactive sorption sites for intermediates [16,17].

Fig. 2(c) and (d) presents the generation and further degradation process of p- and o-CP during the same reaction period with different Pd/Fe nanoparticles prepared in the presence and absence of ultrasound. The experimental results demonstrated that the generation of o-CP was more than that of p-CP, although in the further reductive degradation process, o-CP was easily reduced to phenol appreciably than p-CP. So the concentration of o-CP is much higher than the concentration of p-CP during the reductive dechlorination of 2,4-DCP. The maximum concentrations of o-CP were 4.13 and 4.36 mg L^{-1} with different Pd/Fe nanoparticles prepared

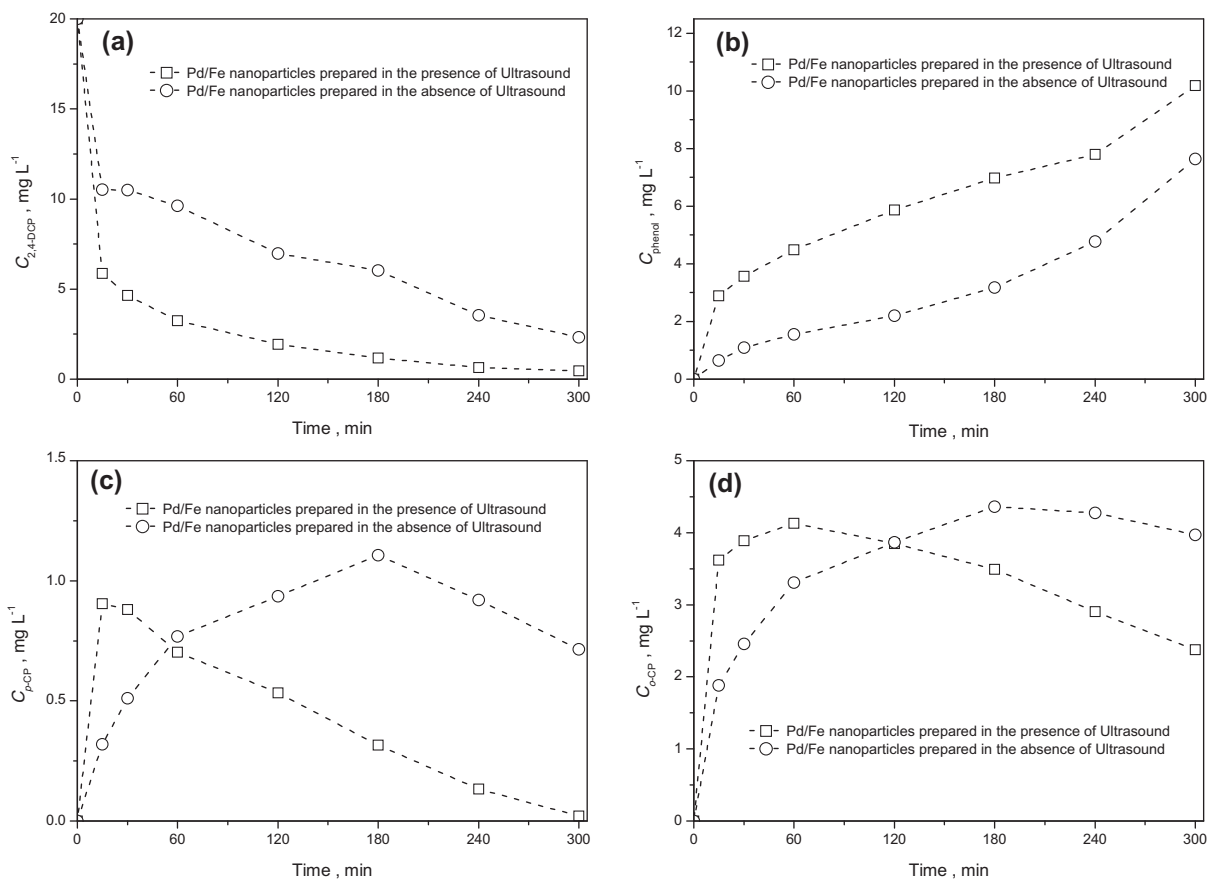


Fig. 2. Dechlorination of 2,4-DCP by Pd/Fe nanoparticles prepared in the presence and absence of ultrasonic irradiation ($T = 25\text{ }^{\circ}\text{C}$, $\text{pH}_{\text{in}} = 3.0$, $C_{2,4\text{-DCP}} = 20\text{ mg L}^{-1}$, $C_{\text{Pd/Fe}} = 3\text{ g L}^{-1}$, mechanical stirring speed at 400 rpm, the Pd loading percentage over Fe^0 was 0.3 wt.%).

in the presence and absence of ultrasound in 60 and 180 min, respectively. The maximum concentrations of o-CP appears to be delayed with Pd/Fe nanoparticles prepared in the absence of ultrasound, but for p-CP, the maximum concentrations were just 0.90 and 1.11 mg L^{-1} in 15 and 180 min, respectively, much less than those of o-CP. Obviously, the catalytic degradation process quickly proceeded with Pd/Fe nanoparticles prepared in the presence of ultrasound than with Pd/Fe nanoparticles prepared in the absence of ultrasound. During the catalytic degradation process, most 2,4-DCP were first transformed into o-CP and p-CP then reduced rapidly to phenol. This was evident from the concentration changing during the reduction of 2,4-DCP, while more and more phenol was produced. However, the concentration of o-CP and p-CP were initially increased in the prophase reaction, followed by a slow decrease. Therefore, Pd/Fe nanoparticles were prepared by using ultrasound strengthened liquid phase reductive method in the following experiments.

3.3. Effects of Pd loading percentage over Fe^0 on 2,4-DCP dechlorination

It has been elucidated that zero-valent iron can promote a hydrogenolysis reaction where a chlorine atom in the organic chlorinated compounds is replaced by a hydrogen atom. Palladium is a well-known catalyst for the hydrogenolysis. Co-existence of palladium and iron in the particles has been proved to be very effective to accelerate the dechlorination reaction. Therefore, the Pd loading percentage over Fe^0 on Pd/Fe nanoparticles may be one of the important influential factors on the dechlorination efficiency. As

Fig. 3 shows the efficiencies of dechlorination and phenol formations were significantly increased as Pd loading percentage over Fe^0 increased from 0.20 to 0.30 wt.%. The removal percentage of 2,4-DCP reached from 64 to 92% within 240 min. The increase in the Pd loading percentage over Fe^0 from 0.3 to 0.4 wt.% only caused slight improvement to the 2,4-DCP dechlorination efficiency. The most likely explanation for this is that the maximum Pd coverage is less than one layer, and in this way, the loss of available catalytic reactive sites due to the overlapping between Pd atoms can be excluded. Nonetheless, the amount of hydrogen gas absorbed by Pd atoms increased with the increasing Pd loading percentage over Fe^0 [19,20], and so make it possible to improve the efficiencies of dechlorination and phenol formations. The slight improvement of the removal efficiency at Pd loading percentage over $\text{Fe}^0 > 0.30$ wt.% is that the accumulation of excessive hydrogen gas hinders the contact between target pollutant and metal particles, and reduces the surface area available for 2,4-DCP dechlorination. This phenomenon is in agreement with previously reported studies [1,17,18]. Pd loading percentage over Fe^0 in Pd/Fe nanoparticles was selected at about 0.30 wt.% for efficient reductive dechlorination and yet minimal palladium usage.

3.4. Effects of Pd/Fe nanoparticles dosage on 2,4-DCP dechlorination

Since the catalytic reductive dechlorination by Pd/Fe nanoparticles takes place on the surface of nanoparticles, therefore Pd/Fe nanoparticles to 2,4-DCP ratio ($\text{g Pd/Fe nanoparticles / mg 2,4-DCP}$) is also a significant influential parameter. The quantity of available surface area is among the most significant experimental

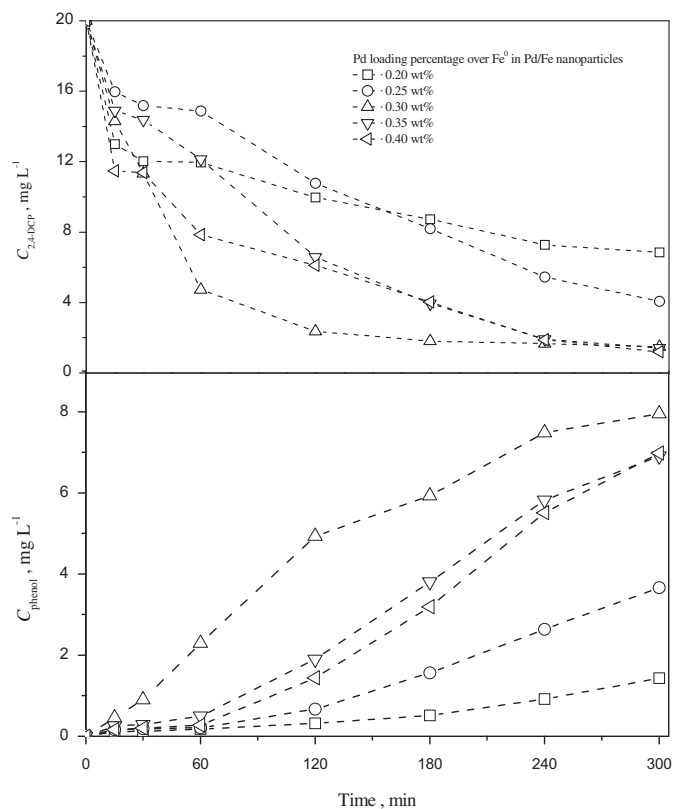


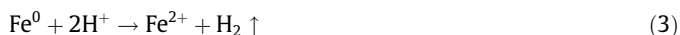
Fig. 3. Effects of Pd loading percentage over Fe^0 in Pd/Fe nanoparticles on 2,4-DCP dechlorination by Pd/Fe nanoparticles prepared in the presence of ultrasonic irradiation ($T = 25\text{ }^\circ\text{C}$, $\text{pH}_{\text{in}} = 5.0$, $C_{2,4\text{-DCP}} = 20\text{ mg L}^{-1}$, $C_{\text{Pd/Fe}} = 3\text{ g L}^{-1}$, mechanical stirring speed at 400 rpm).

variables affecting 2,4-DCP reductive dechlorination reaction. With increasing the concentration of Pd/Fe nanoparticles in the solution, it is insignificant to the final removal efficiency in excess of Pd/Fe nanoparticles dosage. However, it will accelerate the initial reaction rate and provide more active sites of Pd/Fe nanoparticles for collision with 2,4-DCP during the reductive process. Effects of different Pd/Fe nanoparticles dosage on 2,4-DCP dechlorination were explored as shown in Fig. 4. With the elevation of the Pd/Fe nanoparticles dosage from 2 to 6 g L^{-1} , obvious differences were observed, the removal percentage of 2,4-DCP increased from 62% to 94% after 120 min of the reaction. Increasing the dosage of Pd/Fe nanoparticles means the larger Pd/Fe nanoparticles surface area. The higher the Pd/Fe nanoparticles surface area concentration is, the faster the reaction velocity. The removal percentage of 2,4-DCP is similar for a dosage of Pd/Fe nanoparticles of 3 or 4 g L^{-1} after 300 min of the reaction. Hence, the appropriate dosage of Pd/Fe nanoparticles in the level of 3 g L^{-1} is chosen for 2,4-DCP dechlorination.

3.5. Effects of the initial pH value on 2,4-DCP dechlorination

Initial pH value in aqueous solution is an important influential factor in reductive dechlorination of chlorinated organic compounds using ZVI. Different corrosion reactions of iron in acidic and weak acidic or neutral solutions were given below:

Acidic condition:



Weak acidic or neutral condition:

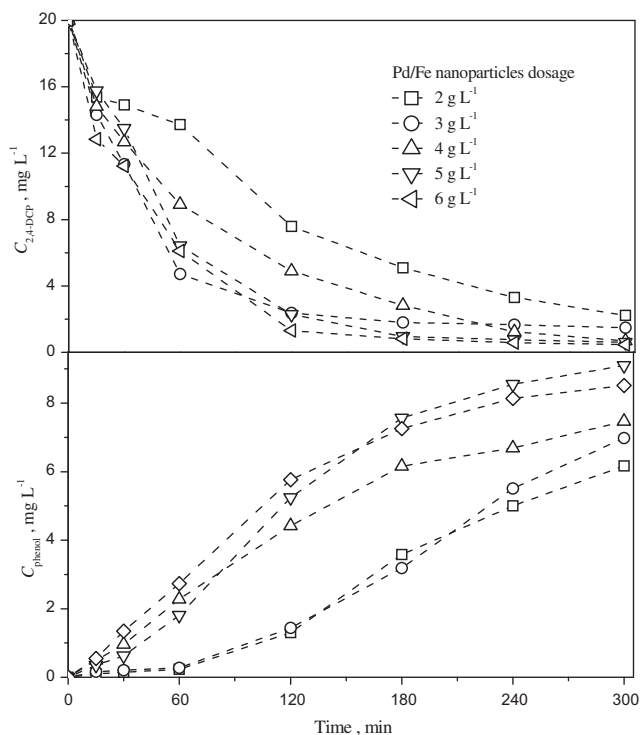
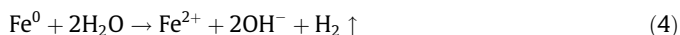


Fig. 4. Effects of Pd/Fe nanoparticles dosage on 2,4-DCP dechlorination ($T = 25\text{ }^\circ\text{C}$, $C_{2,4\text{-DCP}} = 20\text{ mg L}^{-1}$, mechanical stirring speed at 400 rpm, $\text{pH}_{\text{in}} = 5.0$, the Pd loading percentage over Fe^0 was 0.3 wt.%).

Low pH favors more iron surface available for reaction with the chlorinated molecules or at least promote the corrosion rate, leading to release of chloride ions. However, when oxygen was present in the reaction solution, the corrosion product, OH^- , was generated. Therefore, the solution pH should increase even if the initial pH is low. At higher pH values, carbonate and hydroxide coatings undoubtedly develop, which inhibit further decomposition of iron surface and hinder access to the Fe^0 surface. As a result, the catalytic activity decreases. Fig. 5 shows the effect of different initial pH values on the reductive dechlorination of 2,4-DCP by Pd/Fe nanoparticles. Prior to initializing reaction all reactant solutions were adjusted to different pH values by dilution with sulfuric acid (H_2SO_4) and sodium hydroxide (NaOH), and during the reaction pH values were not adjusted. When the initial pH values increased from 3, 5, 7 to 9, the removal percentages of 2,4-DCP dropped from nearly 97%, 96%, 93% to 75%, respectively in 240 min. The increase of initial pH values of the reactant solutions from 7 to 9, leads to the reactant solution change from acidic to alkaline condition, consequently the removal percentages of 2,4-DCP dropped obviously. It indicates that the presence of H^+ largely enhances the 2,4-DCP reductive dechlorination efficiency. The possible reasons may be that (1) the surface of Pd/Fe nanoparticles would be oxidized inevitably during the preparation and storage, which had been demonstrated by the earlier published literatures [21]. However, at lower pH values, the oxides on the particles surface were dissolved, and the active sites of the particle surface were exposed; (2) at lower pH values, the iron corrosion could be accelerated, producing enough hydrogen (or hydrogen atoms), which were in favor of hydrogenation reaction [22,23]; (3) iron corrosion in solution of pH higher than 7 tends to form a passive film of iron oxides and hydroxide on the iron surface, which inhibits further reaction. In the previous study [17], detection of the solution pH during the entire period of the reaction, and ferrous ions/total iron ions produced in the reaction could further support our assumptions.

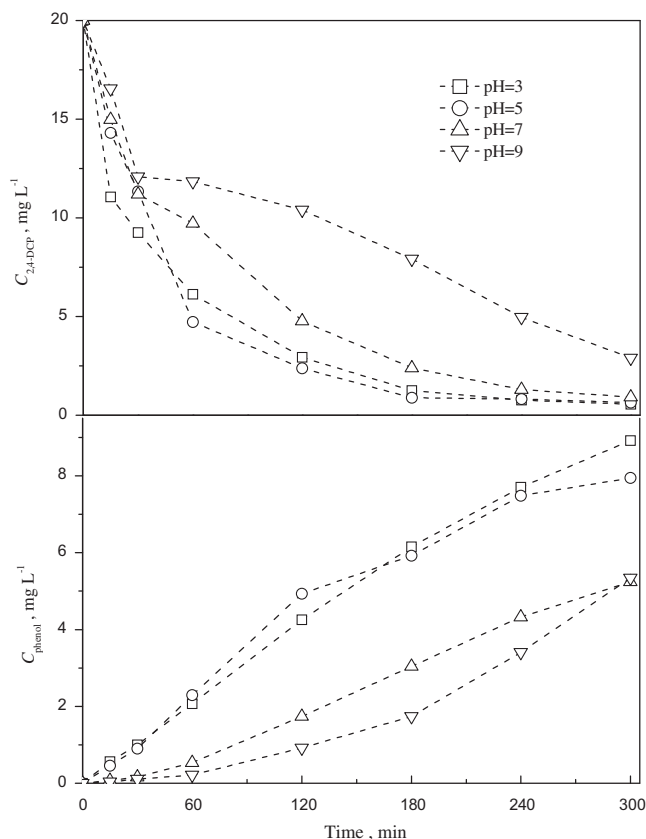


Fig. 5. Effects of solution initial pH on 2,4-DCP dechlorination ($T = 25\text{ }^{\circ}\text{C}$, $C_{2,4\text{-DCP}} = 20\text{ mg L}^{-1}$, mechanical stirring speed at 400 rpm, $\text{pH}_{\text{in}} = 3.0$, the Pd loading percentage over Fe^0 was 0.3 wt.%, $C_{\text{Pd/Fe}} = 3\text{ g L}^{-1}$).

3.6. Effects of mechanical stirring speed on 2,4-DCP dechlorination

Previous studies have reported that the reductive dechlorination of 2,4-DCP by Pd/Fe nanoparticles involves three main steps [1–3,5–10]: (1) 2,4-DCP in aqueous solution diffuse to the Pd/Fe nanoparticles surface and adsorb in the surface of Pd/Fe nanoparticles; (2) the adsorbed 2,4-DCP takes reduction reaction under the effect of Pd/Fe nanoparticles; (3) the products of reaction desorbs from the Pd/Fe nanoparticles and diffuses to the bulk solution. The reductive dechlorination rate is controlled by mass transfer if Pd/Fe nanoparticles dosage is excessive in the reaction. Therefore, the mechanical stirring speed will significantly affect the reductive dechlorination efficiency. Fig. 6 shows the effect of different mechanical stirring speed on the dechlorination of 2,4-DCP by Pd/Fe nanoparticles. When the mechanical stirring speed increased from 200, 400 to 600 rpm, the removal percentages of 2,4-DCP increased from nearly 78, 96 to 99%, respectively in 240 min. With increasing the mechanical stirring speed, it is significant to improve the final removal efficiency because of coupling with the greater mass transfer rate. Hence, the appropriate mechanical stirring speed in the level of 600 rpm is chosen for 2,4-DCP dechlorination.

3.7. Effects of initial 2,4-DCP concentration on 2,4-DCP dechlorination

Five different initial 2,4-DCP concentrations (10, 20, 30, 40 and 50 mg L^{-1}) were employed. Fig. 7 shows the 2,4-DCP reductive profiles with different initial 2,4-DCP concentrations. The removal rates of 2,4-DCP reached 82%, 89%, 74%, 64%, and 71% each after 60 min, and then reached 98%, 99%, 99%, 98%, and 97%, respectively after 300 min of the reaction. Though the final removal percentage

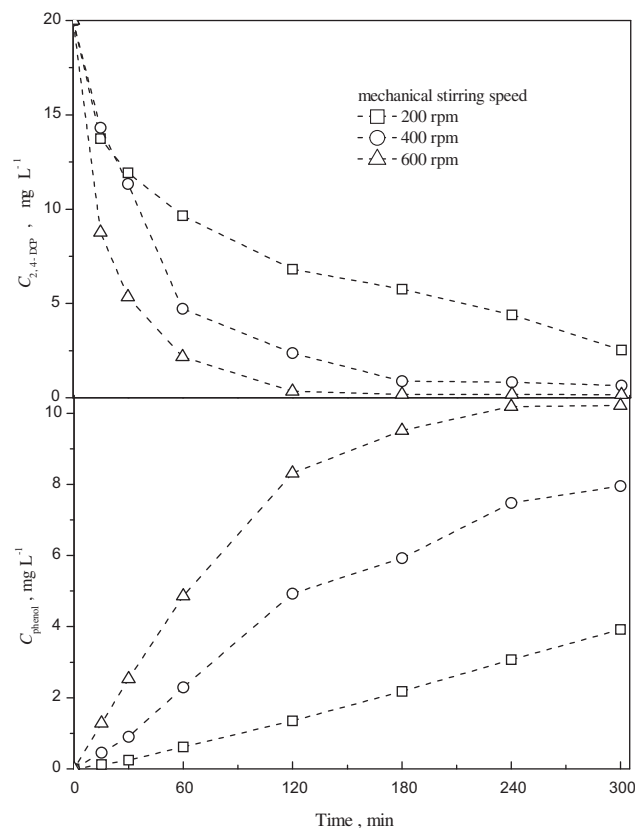


Fig. 6. Effects of mechanical stirring speed on 2,4-DCP dechlorination ($T = 25\text{ }^{\circ}\text{C}$, $C_{2,4\text{-DCP}} = 20\text{ mg L}^{-1}$, $\text{pH}_{\text{in}} = 3.0$, the Pd loading percentage over Fe^0 was 0.3 wt.%, $C_{\text{Pd/Fe}} = 3\text{ g L}^{-1}$).

of 2,4-DCP was close to each other, the absolute removal amount increased with increasing initial 2,4-DCP concentrations.

3.8. Kinetic modeling of 2,4-DCP reductive dechlorination by Pd/Fe nanoparticles

Fig. 2 shows the hypothetical transformation pathways of 2,4-DCP. The products consist of phenol, p-CP and o-CP, so it is assumed that 2,4-DCP was hydro-dechlorinated according to the following sequence of steps. In the following equations, 2,4-DCP, CP and P are the abbreviated forms of 2,4-dichlorophenol, chlorophenol, and phenol, respectively:



where CP represents the total molecules of o-CP and p-CP in the reaction. It is well established that the pseudo-first-order kinetics could be applied in the reductive dechlorination of chlorinated organics by the bimetallic nanoparticles if the bimetallic nanoparticles dosage is excessive in the reaction [1,3,7]. Therefore, the pseudo-first order reaction kinetics was adopted to model the 2,4-DCP dechlorination reaction by Pd/Fe nanoparticles prepared in the presence of ultrasonic irradiation. The corresponding reaction rate equations for the disappearance of 2,4-DCP, the transient formation of CP (including o-CP and p-CP) intermediates, and the accumulation of P in the batch system are shown as follows:

$$-\frac{dC_{2,4\text{-DCP}}}{dt} = k_1 C_{2,4\text{-DCP}} \quad (6)$$

$$\frac{dC_{\text{CP}}}{dt} = k_1 C_{2,4\text{-DCP}} - k_2 C_{\text{CP}} \quad (7)$$

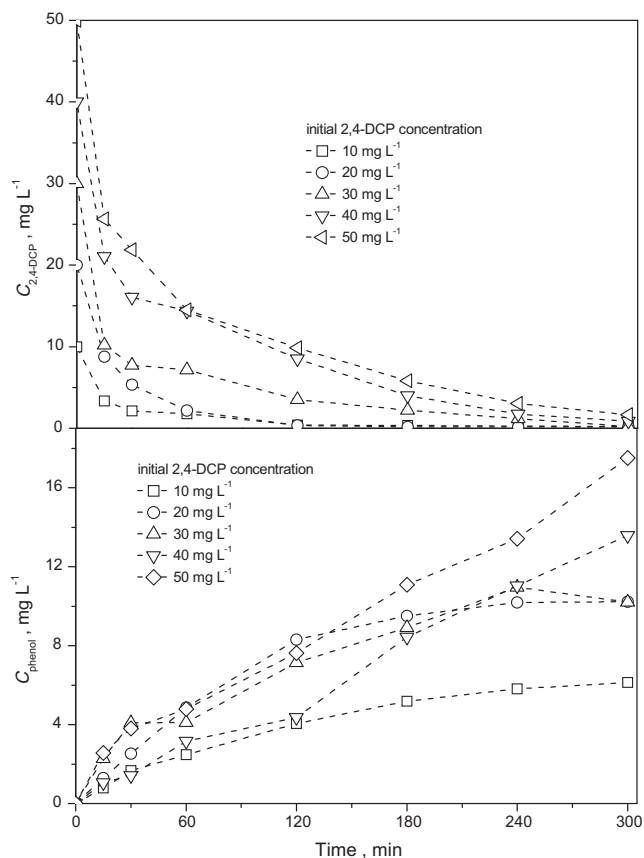


Fig. 7. Effects of initial 2,4-DCP concentration on 2,4-DCP dechlorination ($T = 25\text{ }^{\circ}\text{C}$, $\text{pH}_{\text{in}} = 3.0$, mechanical stirring speed at 600 rpm, the Pd loading percentage over Fe^0 was 0.3 wt.%, $C_{\text{Pd/Fe}} = 3\text{ g L}^{-1}$).

$$\frac{d[\text{P}]}{dt} = k_2 C_{\text{CP}} \quad (8)$$

The above simultaneous rate equations are integrated, leading to the following molar fractions:

Table 1
 k values in different experimental conditions.

Reaction conditions	$1 - a$	k_1/min^{-1}	R	k_2/min^{-1}	R	
Pd/Fe nanoparticles prepared method	In the absence of ultrasound	0.948	0.00786	0.98	0.00613	0.97
	In the presence of ultrasound	0.991	0.04130	0.97	0.00777	0.96
Pd loading percentage over Fe^0	0.20 wt.%	0.968	0.00425	0.94	0.00106	0.97
	0.25 wt.%	0.934	0.00486	0.97	0.00320	0.99
	0.30 wt.%	0.954	0.00826	0.97	0.00430	0.99
	0.35 wt.%	0.941	0.00940	0.98	0.00556	0.99
	0.40 wt.%	0.963	0.01074	0.96	0.00405	0.97
Pd/Fe dosage	2 g L^{-1}	0.948	0.00722	0.98	0.00545	0.99
	3 g L^{-1}	0.954	0.00826	0.97	0.00430	0.99
	4 g L^{-1}	0.946	0.01206	0.99	0.00790	0.94
	5 g L^{-1}	0.957	0.01676	0.99	0.00960	0.99
	6 g L^{-1}	0.969	0.02028	0.99	0.00976	0.98
Initial pH values	3	0.920	0.02101	0.96	0.00726	0.99
	5	0.996	0.02073	0.99	0.00549	0.98
	7	0.906	0.01196	0.99	0.00341	0.97
	9	0.965	0.00572	0.96	0.00405	0.96
Mechanical stirring speed	200 rpm	0.942	0.00277	0.94	0.00277	0.99
	400 rpm	0.954	0.02073	0.99	0.00549	0.98
	600 rpm	0.985	0.04678	0.96	0.01338	0.98
Initial 2,4-DCP concentration	10 mg L^{-1}	0.979	0.05767	0.95	0.01546	0.98
	20 mg L^{-1}	0.985	0.04678	0.99	0.01321	0.98
	30 mg L^{-1}	0.984	0.05872	0.95	0.01516	0.97
	40 mg L^{-1}	0.917	0.02036	0.97	0.0353	0.99
	50 mg L^{-1}	0.989	0.02055	0.97	0.00908	0.98

Note: $1 - a$ represents the molar fraction of the total organic compounds in solution; k_1 and k_2 refer the corresponding reaction rate for the disappearance of 2,4-DCP and CP, respectively; R denotes the correlation coefficient between the experimental data can match the calculated number.

$$\alpha_{2,4\text{-DCP}} = e^{-k_1 t} \quad (9)$$

$$\alpha_{\text{CP}} = \frac{k_1}{k_2 - k_1} (e^{-k_1 t} - e^{-k_2 t}) \quad (10)$$

$$\alpha_{\text{P}} = 1 - \alpha_{2,4\text{-DCP}} - \alpha_{\text{CP}} \quad (11)$$

where α represents the molar fraction of the subscript compound to the initial concentration of the parent compound (i.e., 2,4-DCP). Since a fraction of organic compounds were adsorbed on the larger surface of Pd/Fe nanoparticles, the actual concentration of the organic compound in aqueous phase has to be revised. As the production of P was step wise, equilibrium time for organic compounds adsorbed onto Pd/Fe nanoparticles was little, and the total molar fraction of the organic compounds did not change, the proportion of P in the aqueous phase can be seen as invariable, as a result, Eq. (11) can be revised as follows:

$$\alpha'_p = \alpha_p \times (1 - a) \quad (12)$$

where α' represents the actual molar fraction of the subscript compound to the initial concentration of the parent compound, and a represents the molar fraction of the organic compounds which were adsorbed onto Pd/Fe nanoparticles to the initial concentration of the parent compound (i.e., 2,4-DCP). Then k values were derived from fitting the experimental data into Eq. (12) according to the non-linear least-square regression.

k values in different reaction conditions were listed in Table 1. It shows that k values increased obviously from 0.000786 to 0.0413 min^{-1} under Pd/Fe nanoparticles prepared in the absence and presence of ultrasonic irradiation, respectively. And they increased from 0.00425, 0.00486, 0.00826, 0.00940 to 0.01074 min^{-1} as the Pd loading percentage over Fe^0 in Pd/Fe nanoparticles was increased from 0.20, 0.25, 0.30, 0.35 to 0.40 wt.%. In short, k values increased with the increasing Pd/Fe nanoparticles dosage and mechanical stirring speed, with the decrease of pH values, and k values have nothing to do with the initial 2,4-DCP concentration.

4. Conclusion

Our experimental results suggest that the synthesized Pd/Fe nanoparticles using ultrasound strengthened liquid phase reductive method was a better technique to enhance the dispersion and avoid the agglomeration. In the reductive dechlorination of 2,4-DCP, the dechlorination efficiency was dependent on a number of factors including Pd/Fe availability, mechanical stirring speed, and initial pH values. The degradation of 2,4-DCP followed pseudo-first-order kinetics reaction and the apparent pseudo-first-order kinetics constants were obtained.

Acknowledgements

The authors are grateful for the financial support provided by Zhejiang Provincial Natural Science Foundation of China (No. Y5100075) and by the Science and Technology Department of Zhejiang Province (No. 2012C23044).

References

- [1] Z. Zhang, Q.H. Shen, N. Cissoko, J.J. Wo, X.H. Xu, *J. Hazard. Mater.* 182 (2010) 252–258.
- [2] R. Cheng, J.L. Wang, W.X. Zhang, *J. Hazard. Mater.* 144 (2007) 334–339.
- [3] T. Zhou, Y.Z. Li, T.T. Lim, *Sep. Purif. Technol.* 76 (2010) 206–214.
- [4] A. Vallecillo, P.A. Garcia-Encina, M. Pena, *Water Sci. Technol.* 40 (1999) 161–168.
- [5] J.D. Praveena, K. Palanivelu, *J. Environ. Sci.* 24 (4) (2012) 765–773.
- [6] Y. Fang, S.R. Al-Abed, *Appl. Catal. B* 78 (2007) 371–380.
- [7] J. Wei, X. Xu, Y. Liu, D. Wang, *Water Res.* 40 (2006) 348–354.
- [8] G.V. Lowry, M. Reinhard, *Environ. Sci. Technol.* 35 (2001) 696–702.
- [9] H.L. Lien, W.X. Zhang, *Colloid Surf. A* 233 (2001) 103–112.
- [10] W.H. Zhang, X. Quan, J.X. Wang, Z.Y. Zhang, S. Chen, *Chemosphere* 65 (2006) 58–64.
- [11] K.S. Suslick, M. Fang, T. Hyeon, *J. Am. Chem. Soc.* 118 (1996) (1961) 11960–11961.
- [12] C.Y. Wang, Z.Y. Chen, *Chin. J. Chem. Phys.* 12 (1999) 670–674.
- [13] X.T. Yu, R.H. Teng, R.Z. Hu, *Powder Metall. Technol.* 10 (1992) 136–141.
- [14] D.H. Phillips, B. Gu, D.B. Watson, Y. Roh, L. Liang, S.Y. Lee, *Environ. Sci. Technol.* 34 (2000) 4169–4176.
- [15] Y.H. Huang, T.C. Zhang, *Water Res.* 40 (2006) 3075–3082.
- [16] D.R. Burris, T.J. Campbell, V.S. Manoranjan, *Environ. Sci. Technol.* 29 (1995) 2850–2855.
- [17] Z. Zhang, N. Cissoko, J.J. Wo, X.H. Xu, *J. Hazard. Mater.* 165 (2009) 78–86.
- [18] X.Y. Wang, C. Chen, H.L. Liu, J. Ma, *Water Res.* 42 (2008) 4656–4664.
- [19] Z.L. Liu, X.Y. Ling, X.D. Su, J.Y. Lee, *J. Phys. Chem. B* 108 (2004) 8234–8240.
- [20] C. Grittini, M. Malcomson, Q. Farnando, N. Korte, *Environ. Sci. Technol.* 29 (1995) 2898–2900.
- [21] J.T. Nurmi, P.G. Tratnyek, V. Sarathy, D.R. Baer, J.E. Amonette, K. Pecher, C.M. Wang, J.C. Linehan, D.W. Matson, R.L. Penn, M.D. Driessen, *Environ. Sci. Technol.* 39 (2005) 1221–1230.
- [22] Y.H. Kim, E.R. Carraway, *Environ. Sci. Technol.* 34 (2000) 2014–2017.
- [23] Y. Liu, G.V. Lowry, *Environ. Sci. Technol.* 40 (2006) 6085–6090.